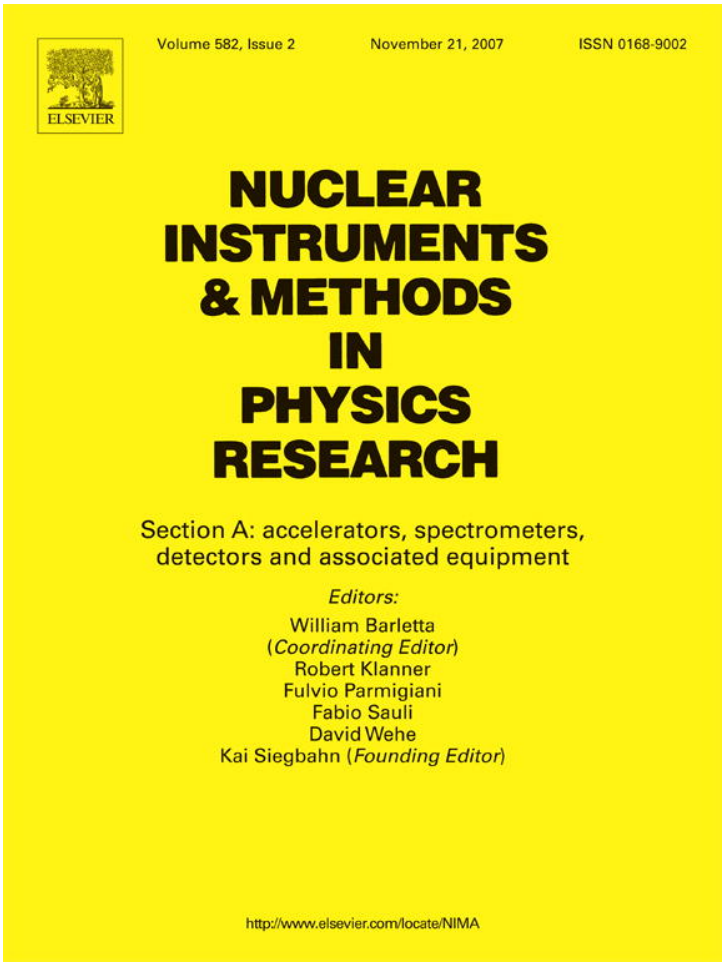

Available online at www.sciencedirect.com
ScienceDirect
Nuclear Instruments and Methods in Physics Research A 582 (2007) 683–692
NUCLEAR INSTRUMENTS & METHODS IN PHYSICS RESEARCH Section A
www.elsevier.com/locate/nima

Inverted pendulum as low-frequency pre-isolation for advanced gravitational wave detectors

A. Takamori[b], P. Raffai[a,*], S. Márka[c], R. DeSalvo[d], V. Sannibale[d], H. Tariq[d], A. Bertolini[e], G. Cella[f], N. Viboud[g], K. Numata[b], R. Takahashi[h], M. Fukushima[h]

[a]*Eötvös Loránd University, Budapest 1117, Hungary*
[b]*The University of Tokyo, Bunkyo, Tokyo 113-0033, Japan*
[c]*Columbia University in the City of New York, New York, NY 10027, USA*
[d]*California Institute of Technology, Pasadena, CA 91125, USA*
[e]*Deutsches Elektronen-Synchrotron, Hamburg 22607, Germany*
[f]*Dipartmento di Fisica, Universita' di Pisa, Pisa, Italy*
[g]*Institut National des Sciences Apliquee at Lyon, Lyon, France*
[h]*National Astronomical Observatory of Japan, Mitaka, Tokyo 181-8588, Japan*

Received 7 June 2007; received in revised form 8 August 2007; accepted 8 August 2007
Available online 19 August 2007

Abstract

We have developed advanced seismic attenuation systems for Gravitational Wave (GW) detectors. The design consists of an Inverted Pendulum (IP) holding stages of Geometrical Anti-Spring Filters (GASF) and pendula, which isolate the test mass suspension from ground noise. The ultra-low-frequency IP suppresses the horizontal seismic noise, while the GASF suppresses the vertical ground vibrations. The three legs of the IP are supported by cylindrical maraging steel flexural joints. The IP can be tuned to very low frequencies by carefully adjusting its load. As a best result, we have achieved an ultra low, ~12 mHz pendulum frequency for the system prototype made for Advanced LIGO (Laser Interferometer Gravitational Wave Observatory). The measured quality factor, Q, of this IP, ranging from $Q\sim2500$ (at 0.45 Hz) to $Q\sim2$ (at 12 mHz), is compatible with structural damping, and is proportional to the square of the pendulum frequency. Tunable counterweights allow for precise center-of-percussion tuning to achieve the required attenuation up to the first leg internal resonance (~60 Hz for advanced LIGO prototype). All measurements are in good agreement with our analytical models. We therefore expect good attenuation in the low-frequency region, from ~0.1to ~50 Hz, covering the micro-seismic peak. The extremely soft IP requires minimal control force, which simplifies any needed actuation.

PACS: 04.30.−w; 04.80.Nn; 95.55.Ym; 07.10.Fq; 07.60.Ly

Keywords: Gravitational wave; Seismic; Isolation

1. Introduction

The fundamental requirements and constraints on seismic attenuation systems vary from application to application. The primary seismic isolation systems for GW interferometers, often referred to as pre-isolators, are usually constructed using both active isolation assemblies and by passive attenuation means.

In most cases, the seismic attenuation, applied downstream of the pre-attenuators, relies on multiple passive pendula and spring mirror suspensions [1]. The passive attenuation chains are installed at the quiet point of seismic pre-attenuators. Utilizing various lengths of pendula (30–100 cm long), these chains have several rigid-body resonances between 0.3 and 3 Hz, and typically very large quality factors (Q in the thousands). Inadequate seismic pre-attenuation within this frequency range can allow

*Corresponding author. Department of Atomic Physics, Institute of Physics, Pazmany Peter Setany 1A, 1117 Budapest, Hungary.
Tel.: +1 212 854 8209; fax: +1 212 854 8121.
E-mail address: praffai@bolyai.elte.hu (P. Raffai).

0168-9002/$ - see front matter © 2007 Elsevier B.V. All rights reserved.
doi:10.1016/j.nima.2007.08.161

direct seismic excitation of these resonances. As a result of insufficient pre-attenuation and/or resonance damping, large resonant excursions can occur, overwhelming the payload's (interferometer test mass mirror) position control actuators. As a consequence, the experimenters might be unable to lock their interferometer, or the large oscillations can have detrimental effects on the science reach of the interferometers.

The reduction of the maximum motion, required from the actuators, is also fundamental to reduce the noise introduced by the control system. Therefore, it is of utmost importance to protect the test mass suspensions from excitations in the 0.1–5 Hz frequency band through highly efficient seismic pre-isolators. In addition to direct seismic excitations, the attenuation chain resonances may be excited by the mirror control actuators. In this case, energy stored in the rigid body modes of the mirror multiple pendulum system must be extracted by means of damping. Damping, reducing the low frequency mirror RMS motion, can either be internal to the multiple pendulum system [2–6] or inertial, obtained from the pre-isolator [7–10]. The IP system presented here is intended for use with inertial damping of suspension resonances and is therefore equipped with accelerometers.

Absolute positioning of the mirror suspension end point, with a precision much smaller than a micron over a range of millimeters, is necessary to correct for large ultra-low-frequency perturbations due to tides, daily and seasonal ground tilts and seismic events. This must be accomplished at the pre-attenuator level, without disrupting the mirror's servo systems.

Considering these aspects of seismic isolation of interferometric GW detectors, we have developed advanced Seismic Attenuation System (SAS) prototypes and achieved good seismic attenuation. The fundamentals of SAS are conceptually similar to the super attenuator of Virgo Collaboration while the SAS utilizes novel geometries and high-quality materials. Vibrations in the three horizontal degrees of freedom are effectively pre-attenuated by a tri-legged ultra low-frequency IP table, while the vertical disturbances are attenuated by means of Geometrical Anti-Spring Filters. The two remaining tilt modes are mitigated by the fact, that the chain is suspended by a single thin wire, which is not a good conductor of tilt motion.

SAS is a mainly passive system, which ensures reliable attenuation, is essentially free of external couplings and electronic noise and has little susceptibility to accidental active excitation. Weak active components are employed within the system to keep the system optimally aligned and/or to suppress the internal resonances of the mirror suspension assembly. In the case of the IP table the active components are linear variable differential transformer (LVDT) position sensors, voice coil actuators and highly directional horizontal accelerometers.

This paper is concerned with the horizontal pre-attenuation stage, i.e. the IP table design and performance, presenting the results of two different prototypes and insights for future developments.

Note, that similarly relevant results on passive seismic attenuation were published by the Western Australia University group discussed in Refs.[11–13].

2. The detailed structure of the SAS IP table

The IP is in many ways an ideal system for vibration attenuation in the horizontal plane, in spite of its sensitivity to ground tilts. It allows achievement of very low resonant frequencies, and therefore a large seismic noise attenuation factor, with the simple tuning of its payload weight, permits micro positioning with negligible forces, while obtaining the gain of altitude necessary to suspend the attenuation chain. The large range of motion of the IP pre-isolator provides earthquake protection for events of up to several millimeters of excursion.

In order to create a stable support for the vertical static load, our IP is constructed with three rigid cylindrical legs supporting a rigid table. The use of the tri-legged IP table has the fundamental advantage of providing a platform, which has movements confined in the horizontal plane, while being extremely soft inside that plane (translations and yaw). The property of having only horizontal movements is very important when active controls are applied to provide inertial damping for the attenuation chain resonant modes. Any off-plane actuation force would be neutralized by the system's rigidity. The horizontal accelerometers can be built to be very insensitive to vertical and rotational accelerations, but are intrinsically sensitive to horizontal accelerations and to tilts (equivalence principle).

It is of importance to separate the horizontal degrees of freedom from the vertical ones. In order to avoid translation/tilt couplings, it is very important to construct the IP legs perfectly straight and of identical length. Both requirements can be achieved with machining and assembly precision of less than 0.1 mm.

All three legs of the IP are attached to a platform via identical, precision-machined maraging steel [14] cylindrical flexures, serving as pivot points for the IP and providing the harmonic restoring force to keep the IP table straight up. The reduction of the IP resonant frequency is obtained by taking advantage of the gravitational anti-spring effect

$$k_{\mathrm{grav}} = \frac{mg}{l}$$

where m is the payload mass, l is the IP leg's length, and g is the gravitational acceleration. The spring constant k_{grav} acts with a negative sign (restoring force) for a normal pendulum (load mass below the hinge point) and with a positive sign (repulsive, anti-spring force) for an inverted pendulum with the load above the hinge point.

The flex-joints are calibrated in both diameter and length to generate restoring force slightly over-matching

the anti-spring effect caused by the desired payload. Thin flexures connect the top of each IP leg to the IP table. The top flexures are made of 3 cm long double-nail-head wires mounted between a bridge on the leg's tip and an arm extending from the table. A small amount of ballast load on the table is fine-tuned to achieve the required low resonant frequency.

The ideal IP leg is a mass-less, infinitely stiff leg. Unfortunately, real legs are rods with finite thickness and mass. Due to inertia, a rigid rod that is shaken at one end (like an IP leg shaken by seismic excitation) tends to rotate around its so-called center of percussion [15,16]. Any payload attached at the other end of the rod is therefore counter-shaken, although by a reduced amount. The table of a simple-rod IP would therefore be excited with a reduced motion opposed to the seismic motion. This motion has amplitude proportional to the mass ratio between the leg and its payload, with a coefficient smaller but comparable to 1. This effect limits the performance of IP mechanical isolators.

To circumvent this problem, the legs are made of thin wall pipes to be as light, but still as rigid as possible, and then are equipped with counterweights mounted on a 'bell' extending below the flex-joint. The counterweights are finely tuned to position the legs' center of percussion just on the effective bending point of the flex-joint, thus mitigating the transmission of vibrational energy to the table. Details and methodology of counterweight tuning are discussed later in this paper.

Variations of the ground tilt at frequencies around the IP resonant frequency and below are inherently converted to horizontal motion by the IP, with a large conversion coefficient. A multiple input–multiple output (MIMO) active system with a static position relative to ground control is implemented at very low frequencies, in order to minimize the effects of the low-frequency tilt noise and daily tilt cycles variations. Inertial damping relying on state of the art accelerometers [17] and voice coil actuators [18] can be used to reduce the motion of the payload mechanical resonances. We implemented an active damping scheme (in TAMA-SAS), similar to the one already successfully demonstrated by Virgo [19,20].

The position of the IP system relative to ground is sensed by a set of LVDT position sensors with a typical resolution of 10 nm/sqrt(Hz) at 100 mHz [21]. These sensors, as well as the external interferometer length signals, are used to control the IP positioning. The necessary correction force is provided by the Very Low Frequency Control System (VLFC). The VLFC drives the top of the IP via low noise voice coil actuators [18], developed to provide single axis actuation, while minimizing actuation cross talk between the orthogonal axes and avoiding transduction of seismic excitation of the actuator into force modulation.

A spring–actuator system, consisting of three pairs of very soft coil springs mounted in parallel to the voice coil actuators, relieves the actuators of their static load and maintains the IP table at the desired location even in case of power failure. The springs of each pair are connected in series. The three pairs are mounted tangentially to the periphery of the table to form an equilateral triangle. The mid-point of each pair is attached to three motorized sleds connected to the ground through the top of the safety support structure. Moving the sleds controls the static IP positioning to precisely correct any misalignment or assembly imperfection of the three flex-joints, or small ground tilts. The tuning springs need only to be stiff enough to allow this correction, and generate enough pull to drag the IP over the entire required static positioning dynamic range. It is easily seen, that the lower the IP is tuned in frequency, the less stiffness is required from the springs for positioning, while the flex-joint misalignment correction force requirement remains constant. Typically, because the IP is operated at the lowest possible resonant frequency, correction for flex–joint misalignment will be dominant. Additionally, high precision machining of parts reduces the stiffness requirements of these springs. Normally, less than 100 N/m springs are adequate.

As long as the lower flex-joints are mounted directly below and on the same triangle of the small flex-joints at the top of the legs, and there is only x–y movement, the IP table will move precisely in the horizontal plane. If, for example, the lower flex-joints were to be positioned on a wider or smaller triangle, the IP table would move along a sphere centered at the interception point of the axis of the legs. Unequal triangles would result in movements along saddle surfaces. This "cradle" [10] effect would couple translations to tilts in a manner undistinguishable to any horizontal accelerometer mounted on the table. Similarly, large static yaw or differences in leg lengths can produce worrisome effects.

A procedure was developed to use the top flex-joint emplacements on the IP table to position the lower flex-joint supports within 0.1 mm. Leg lengths' equalities within the same limits can also be achieved by mechanical machining techniques.

Due to the extreme softness of the residual effective spring (~8.5 N/m), the IP requires very small control forces from the coil actuators for tasks like tracking tides and compensating for daily tilts. This simplifies the actuation scheme and minimizes the actuator/electronic noise injected above the control frequency band.

2.1. Center of percussion effect

A simple, idealized model of an IP consists of a payload standing on a leg with its mass and moment of inertia sitting on a flexural joint that produces the restoring force.

The transfer function of this idealized IP behaves similarly to that of the harmonic oscillator [22,15]. While a mass-less oscillator shows unlimited attenuation performance for growing frequencies, the modeled IP transfer function flattens at high frequencies somewhere above its resonant frequency forming a plateau, and the attenuation performance becomes saturated. The saturation behavior is

governed by the so-called 'center of percussion (COP) effect' [15,16,22].

To mitigate the COP effect (i.e. reducing the level of the plateau), the mass distribution of the leg must be arranged that the center of rotation coincides with the payload suspension point. It is normally achieved by extending the leg downwards below the flex-joint and adding a counter-weight (CW). Fig. 1 describes the model of the IP with this CW.

The model is parameterized by the following variables:

l_1—length of the IP leg
m_1—mass of the IP leg
I_1—moment of inertia about the center of mass of the IP leg
M—mass of the payload
l_2—length of the bell
m_2—mass of the bell
I_2—moment of inertia about the center of mass of the bell
M_3—mass of the CW
k_θ—torsional spring constant of the flex-joint
(x,z)—position of the payload
(x_0,z_0)—position of the flex-joint attached to the ground
θ—angle of the IP leg with respect to the vertical axis

In the model with the CW, the equation of motion and the transfer function of the IP are written as

$$-C\omega^2 x - B\omega^2 x_0 = -A(x - x_0)$$

$$H_{\mathrm{IPCW}}(\omega) = \frac{A + B\omega^2}{A - C\omega^2}$$

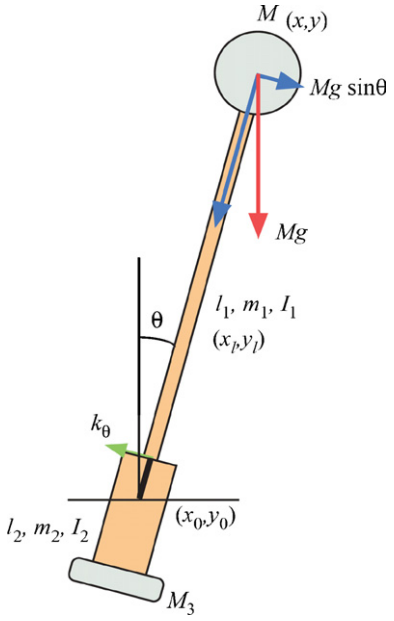

Fig. 1. A schematic view of the IP with the CW mounted at the bottom of the leg. The counter-weight is mounted at the bottom of a bell, coaxially with the leg.

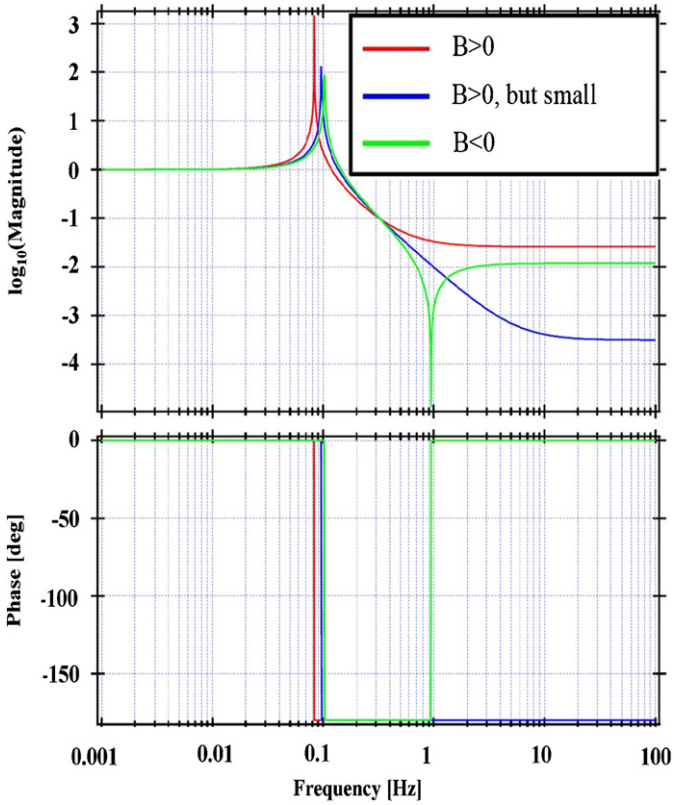

Fig. 2. Transfer function of the IP with excessive (black and grey) and insufficient (light grey) CW. The attenuation performance at high frequencies is substantially improved with a CW close to the ideal one (black).

respectively, where

$$A = \frac{k_\theta}{l_1^2} - \frac{g}{l_1} \times \left(M + \frac{m_1}{2} - \frac{m_2 l_2}{2l_1} - \frac{M_3 l_2}{l_1} \right)$$

$$B = -\frac{I_1 + I_2}{l_1^2} + \frac{m_1}{4} - \frac{m_2 l_2 (2l_1 + l_2)}{4l_1^2} - \frac{M_3 l_2 (l_1 + l_2)}{l_1^2}$$

$$C = M + \frac{m_1}{4} + \frac{m_2 l_2^2}{4l_1^2} + \frac{M_3 l_2^2}{l_1^2} + \frac{I_1 + I_2}{l_1^2}.$$

The plateau level in the transmissibility is determined by B and C. The parameters related to the bell and the CW can be used to maximize attenuation at high frequencies. Particularly, the IP realizes ideal attenuation when B is canceled with the optimal CW.

Too much CW overcompensates the mass of the leg and brings the center of rotation point beyond the tip of the leg. Then the IP leg tip's action has the sign opposite that of the translational motion transmitted by a massless oscillator, and a notch appears in the transfer function when the two amplitudes are the same, as shown in Fig. 2.[1] A leg

[1]Expression of $H_{\mathrm{IPCW}}(\omega)$ holds true between the IP resonant frequency and the first internal mode resonant frequency of the IP leg. Beyond the resonance, the IP leg acts like an elastic element, the compensation mechanism would fail but the leg would provide additional isolation, while degrading the performance at its internal resonant frequency. A leg internal resonance damper may be needed.

under- or over-compensated by the same amount would generate a transmission plateau at the same level, with transmitted motion with the opposite or same direction of the seismic motion respectively. Ref. [10] offers an excellent extended discussion on this topic.

2.2. Quality factor of the IP and effects of damping in the flex-joint

In case of a real IP, inelastic damping effects must also be taken into account. Source of damping can be viscosity of the medium around the IP (viscous damping) and internal energy dissipation in the flex-joint (structural/hysteretic damping). Because the SAS IP is operated at low frequency, viscous damping is negligible even in air.

Assuming that the energy dissipation of the IP is localized in the flex-joint and the origin of the loss is intrinsic of the material, one can introduce [10] an imaginary part with a loss angle ϕ_θ to the torsional spring constant. Thence the effective linear spring constant (for an IP without CW) becomes

$$k'_{\text{eff}} = \frac{k_\theta}{l^2} \times (1 + \mathrm{i}\phi_\theta) - \left(\frac{m}{2} + M\right) \times \frac{g}{l}$$

and one can define the equivalent loss angle of the effective spring constant as

$$\phi_{\text{eff}} = \frac{k_\theta}{l^2 \times k_{\text{eff}}} \phi_\theta.$$

The quality factor of a damped harmonic oscillator is measured as the ratio of the transfer function magnitude at the resonance and that at zero frequency. For an oscillator with only structural damping and no gravitationally stored potential energy, the quality factor is equal to the reciprocal of the material's loss angle ϕ_θ. In the IP case, the effective loss angle is ϕ_{eff}, thus for the quality factor of the IP the following rule applies:

$$Q_{\text{IP}} = \frac{l^2 \times k_{\text{eff}}}{k_\theta} Q_{\text{intrinsic}}$$

where $Q_{\text{intrinsic}}$ is the quality factor originated from the loss angle ϕ_θ.

Note that the quality factor of the IP reduces with the effective spring constant, proportionally to the square of resonant frequency. This is a very important and useful property, because an IP tuned at sufficiently low frequency needs no external damping.

Below the point of $Q \sim 1$ the IP (or any mechanical oscillator-like the GASF, for example, with artificially reduced resonant frequency) becomes hysteresis dominated, and requires an external static positioning compensation system.

3. IP design and measurement methodology

We have designed and fabricated two IP prototypes with very similar structure, but with different size and attenuation properties. A small prototype (with leg length of 1.3 m) was designed to provide a pre-attenuation system for the Japanese detector TAMA300 (IP-TAMA SAS [22,29]). A large prototype (with leg length of 2.6 m, excluding the CW) was designed for a Virgo-like suspension chain intended for Advanced LIGO. We performed a series of experiments to tune and characterize these two IPs. In this section we discuss the details on IP design, the measurement methodology, and results of our experiments.

3.1. Design

The basic requirements for the IP design include isolation requirements as well as practical concerns. There are two critical requirements at low frequency: RMS displacement and velocity of the mirror. They are both dominated by the pre-isolator performance, namely the movement of the resonance of the IP and the 'tail' associated with the suspension chain resonances excited by the residual seismic motion leaking through the pre-isolator. Choosing the right resonant frequency, reducing its quality factor, and generating sufficient low-frequency attenuation are crucial in the IP design.

Approximating the IP attenuation performance with that of the ideal harmonic oscillator (i.e. perfectly tuned CW) and assuming the standard seismic model, yields a requirement for the isolation factor at 1 Hz to be below 1/1000, and for the corresponding resonant frequency f_{IP} to be $<\sim$30 mHz. To realize the requirement of 1/1000 attenuation at 1 Hz we had to reduce the COP plateau to below 60 dB. Although the pre-isolator IP is not required to provide isolation in the detection band, any isolation above 10 Hz is welcome. The plateau extends to the first leg resonant frequency. We designed a large diameter leg with its first resonance at 55 Hz.

For the earlier, taller IP for Advanced LIGO, the goal was to decrease the resonant frequency to the lowest technically achievable value. In that setup we achieved a resonant frequency in the range of 10–20 mHz.

The achieved frequencies have to be regarded as upper limits. The practical limiting factors for the IP resonant frequency tuning are the short-term ground tilt stability, the air current perturbations, and ultimately the material hysteresis.

The tests were made in air in a foil faced foam enclosure to reduce the effect of air currents and fast temperature variations. In-vacuum operation should allow lower IP tuning frequencies.

The design of an IP leg is shown in Fig. 3. Three mechanically identical IP legs are supporting a round-shaped table containing a vertical isolation filter. The connection from the leg to the top table is made via small, soft flex-joint links and the connection between the base plate and the leg's body is made with a stiff flex-joint. The leg bodies are made of thin-wall stainless steel tubes for light-weight and high stiffness, while the flex-joints are made of precipitated Marval 18 maraging steel for high

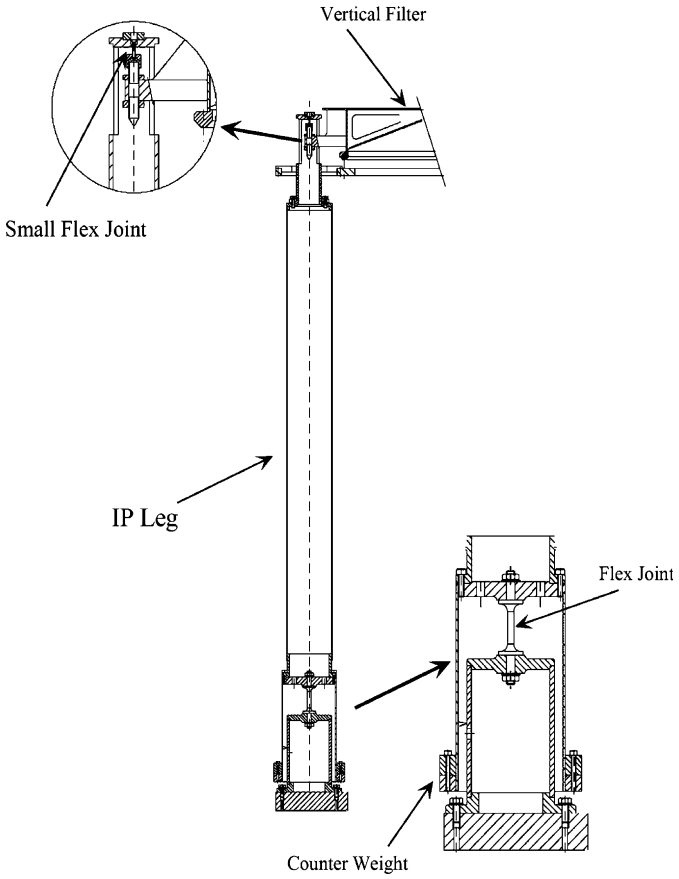

Fig. 3. Design of the prototype IP leg.

elasticity and low creep rate [23,24]. The diameter of the stiff flex-joint is determined such that the spring stiffness matches the stiffness of a pendulum with the IP length and the required payload. Low-frequency IP tuning (see Section 3.2) is then obtained by careful matching of these two stiffnesses.

The design has a large safety margin in terms of buckling. CWs for the COP tuning are secured on the edge of 'bells' bolted to the legs' ends and surrounding the flex-joints.

3.2. Frequency tuning of the IP and internal resonances

It is desired to have the internal resonances of the IP leg well above the bandwidth of the active inertial damping [20] (typically <10 Hz) to avoid saturation of the inertial sensors on the IP and for simplicity of the servo design. All three IP legs of the SAS configuration are identical; therefore, we analyze a single leg. The analysis was done with finite element computations for the Advanced LIGO case and with comparing the simulated results and actual resonance measurements. For IP-TAMA SAS, we simply scaled down the design of the Advanced LIGO prototype. The TAMA IP leg resonances had very similar values.

All the first internal resonances of the pre-prototype IP-Advanced LIGO SAS leg were modeled, subsequently

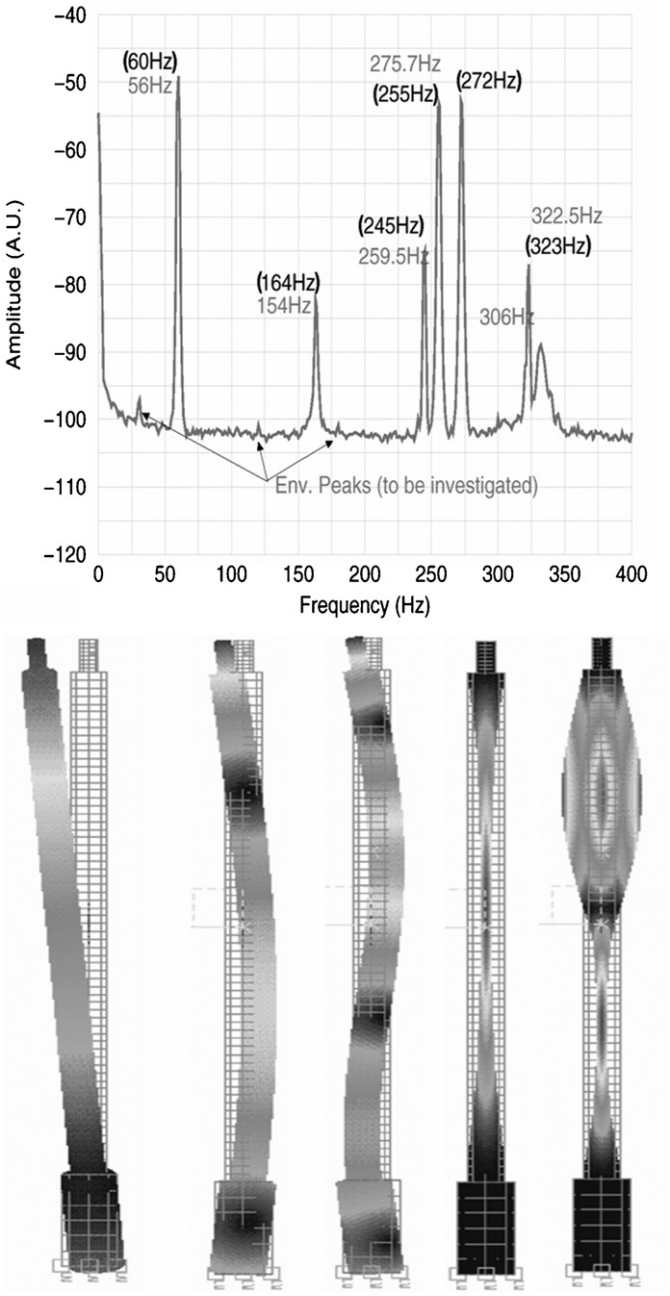

Fig. 4. Internal resonances of the Advanced LIGO prototype IP leg. Grey numbers refer to ANSYS simulation, while black, bracketed numbers to the measurement.

measured and identified, as illustrated in Fig. 4. The calculated resonance frequency values were always within less than ~10% of the measured ones. The lowest resonance was found around 60 Hz for a free-standing leg. For IP-TAMA SAS, we obtained the first resonance at ~50 Hz. Having the first resonance above 50 Hz for the IP legs is a significant improvement from the similarly designed IP in Virgo, which had the first resonance at 9 Hz.

Part of the improvement comes from shorter monolithic legs, without massive flanges along the length, and partly from the usage of larger diameter tubes.

In order to tune the IP prototypes to achieve the lowest external resonant frequency and to determine its required payload mass, we measured the IP resonant frequency as a function of its payload. The results are plotted in Fig. 5 for both IP prototypes.

For IP-TAMA SAS, the minimum resonant frequency measured through the tuning is about 25 mHz and the target frequency of 30 mHz is achieved with the payload of about 160 kg on three legs. Also by fitting the measured curve with the model described in Section 2.1, the parameters of the IP table can be determined. The small differences are attributed to differences between the actual dimensions and the dimensions in the drawings, and to simplification in the model.

We were able to tune the resonance frequency of the lowest frequency radial modes of the IP (i.e. leaning motion of the IP legs towards the center vertical axis of the IP table) for Advanced SAS to as low as ~12 mHz.

These low-resonant frequencies have been achieved in air, despite the substantial atmospheric perturbation of the room. In order to reach these low frequencies, we had to build a rigid hut around the IP, to mitigate the varying airflow due to air conditioning.

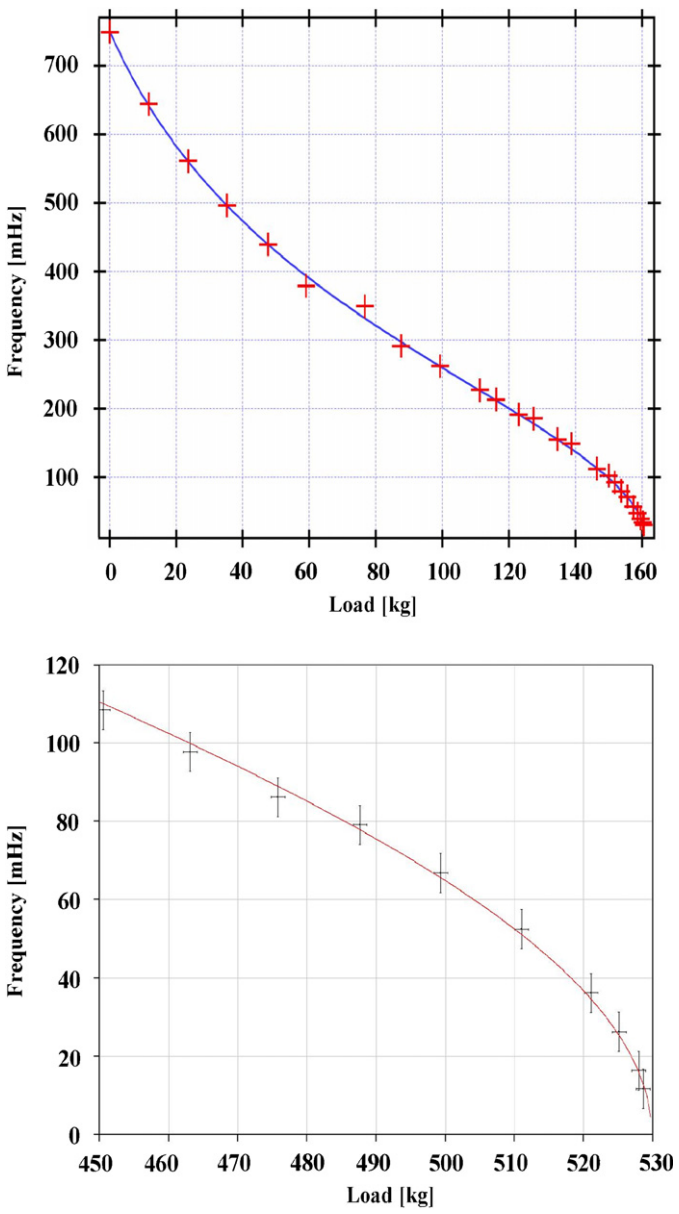

Fig. 5. Load and the resonant frequency of IP-TAMA SAS (top) and IP-Advanced SAS (bottom). Continuous curves show fits using simple theoretical model discussed in Section 2.1. Loads have uncertain offset due to the uncertainties of the weight of the largest masses and error accretion over many smaller ones.

3.3. Reduction of quality factor

We measured the oscillation quality factor as a function of frequency. The relation of the quality factor versus the IP frequency is shown in Fig. 6. The quality factor follows a quadratic function of the resonant frequency, as discussed in Section 2.2. The result is compatible with structural damping.

3.4. Counter weight tuning: isolation performance measurements

Detailed CW tuning measurements were only performed for IP-TAMA SAS.

The coaxial counter-weight that allows positioning of the leg's percussion point over its top flex-joint effective bending point is obtained by extending a section of larger diameter pipe around and below the bottom flex-joint and mounting tunable masses at its lower end. This solution preserves the leg's cylindrical symmetry. In order to measure the IP performance as a function of CW tuning; it was necessary to shake the bottom of the IP in the horizontal plane, at low frequency and with large amplitudes. For this we mounted the IP prototype on a custom shaker.

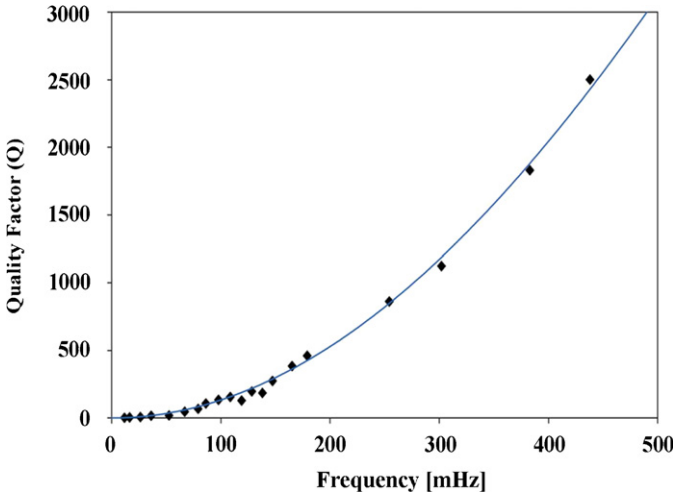

Fig. 6. Measured quality factor versus resonant frequency of IP-Advanced LIGO SAS.

The shaker consists of an oil-bearing system supporting the IP structure and a voice coil exciter connected to it. The IP base is mounted on three oil-bearing units, and is connected to the ground by retainer springs to define the equilibrium position. The motion is constrained to one dimension by a linear slide. One of the oil bearing units is illustrated in Fig. 7. The motion of the IP top table and of the base is detected by commercial low-frequency accelerometers (TEAC 710). The transfer function of the IP is computed in real time by a spectrum analyzer (Stanford Research Institution SR785).

As the CW is decreased, the terms in the expression of $H_{\mathrm{IPCW}}(\omega)$ change from over- to under-compensated. Correspondingly, the IP transfer function improves and then worsens as shown in Fig. 8. We were forced to take the measurements with the IP tuned at 200 mHz (thus hiding most of the attenuation plateau) because the oil-bearing film provided limited vertical stiffness, therefore, not allowing lower frequency tuning. However, the series of measurements with the IP tuned at higher frequency provided good parameter estimations for our model. Thus, we extrapolated the measurements via calculations, based on the validated models.

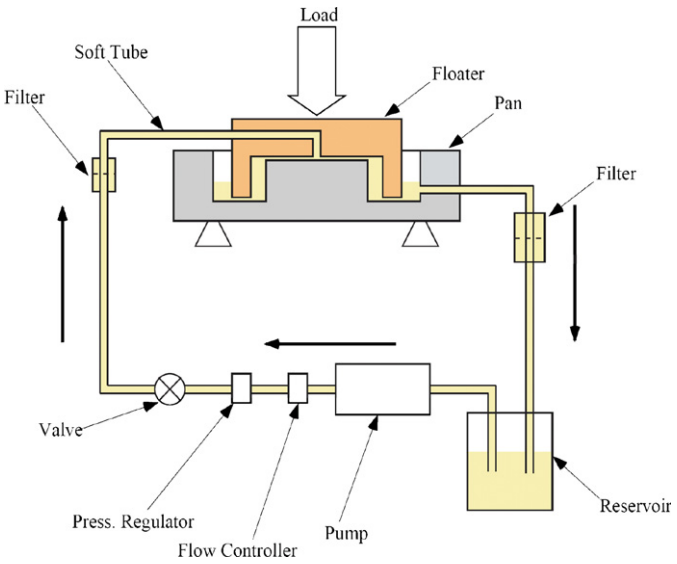

Fig. 7. The oil bearing system. The oil is driven by a pump. Flow and pressure are controlled by regulators. In-line filters were necessary to insure smooth operation. Flexible pipes allowed the movement of parts. The load is supported by a centrally fed brass floater. The oil outflow is collected in a precisely machined oil pan. The resulting thin oil film between the floater and the bottom of the pan sufficiently reduces the friction to allow movements with the small force provided by a voice coil.

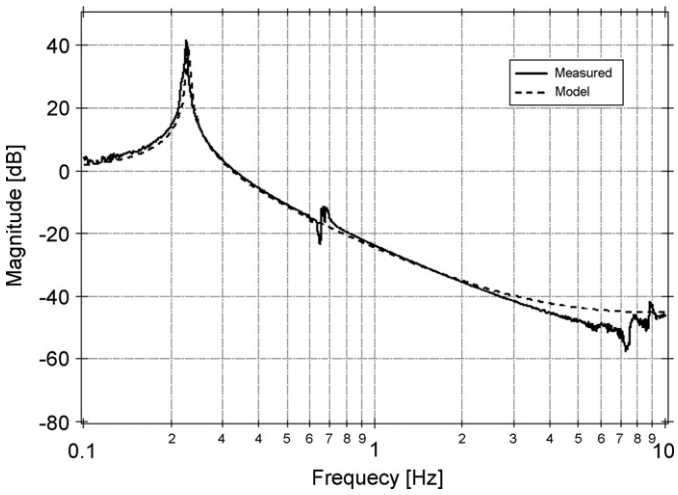

Fig. 9. Horizontal transfer function of the prototype IP TAMA SAS, tuned to 220 mHz. Structure around 650 mHz is caused by cross-coupling from the rotational mode of the IP. The plateau level given at 10 Hz is −47 dB.

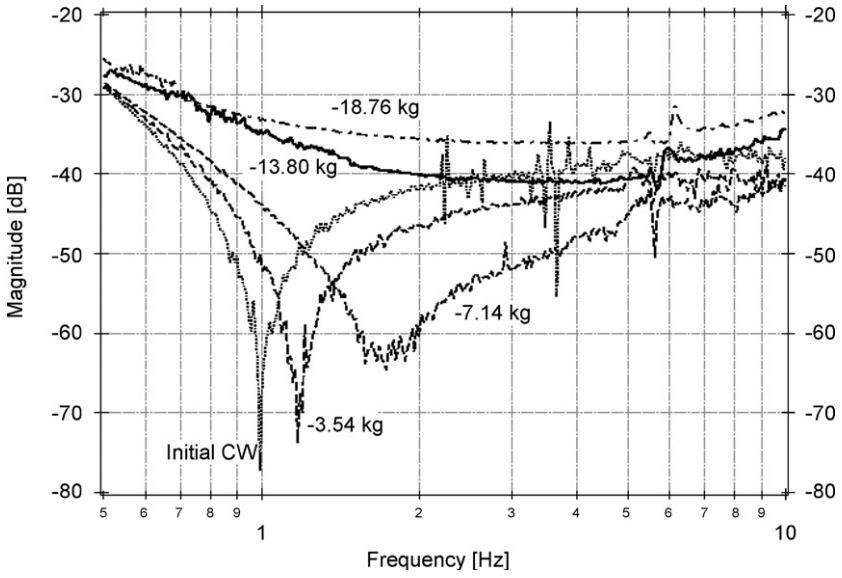

Fig. 8. Plateau level in IP-TAMA SAS transfer function, with various counter weights.

The transfer function of the final IP TAMA SAS prototype is shown in Fig. 9 together with its modeled function (−47 dB at 10 Hz). The attenuation saturation plateau extends up to the first internal mode of the leg, beyond which the leg stops behaving like a rigid body.

4. Conclusions

We have developed and built a high-performance seismic attenuation system, utilizing novel geometries and high-quality materials. The system relies on passive attenuation for frequencies above 0.1 Hz, while active damping of payload resonances is relegated to lower frequencies RMS seismic-noise reduction. We built a proof-of-concept prototype for LIGO and a working Ultra High Vacuum (UHV) compatible system for TAMA (see Fig. 10). We demonstrated that the system is scalable and provides good horizontal attenuation. The IP as well as the novel suspensions that it carries [25–27] were tested in the TAMA 3m interferometer at the University of Tokyo, and they are currently being implemented in the TAMA300 interferometer upgrade [29]. This system is also chosen as the baseline design for the Large Cryogenic Gravitational Wave Telescope (LCGT) [28].

Using the experience gathered in this work, a drastically shorter IP table has been recently designed, and prototyped as a horizontal pre-attenuator for applications in advanced gravitational wave detectors.

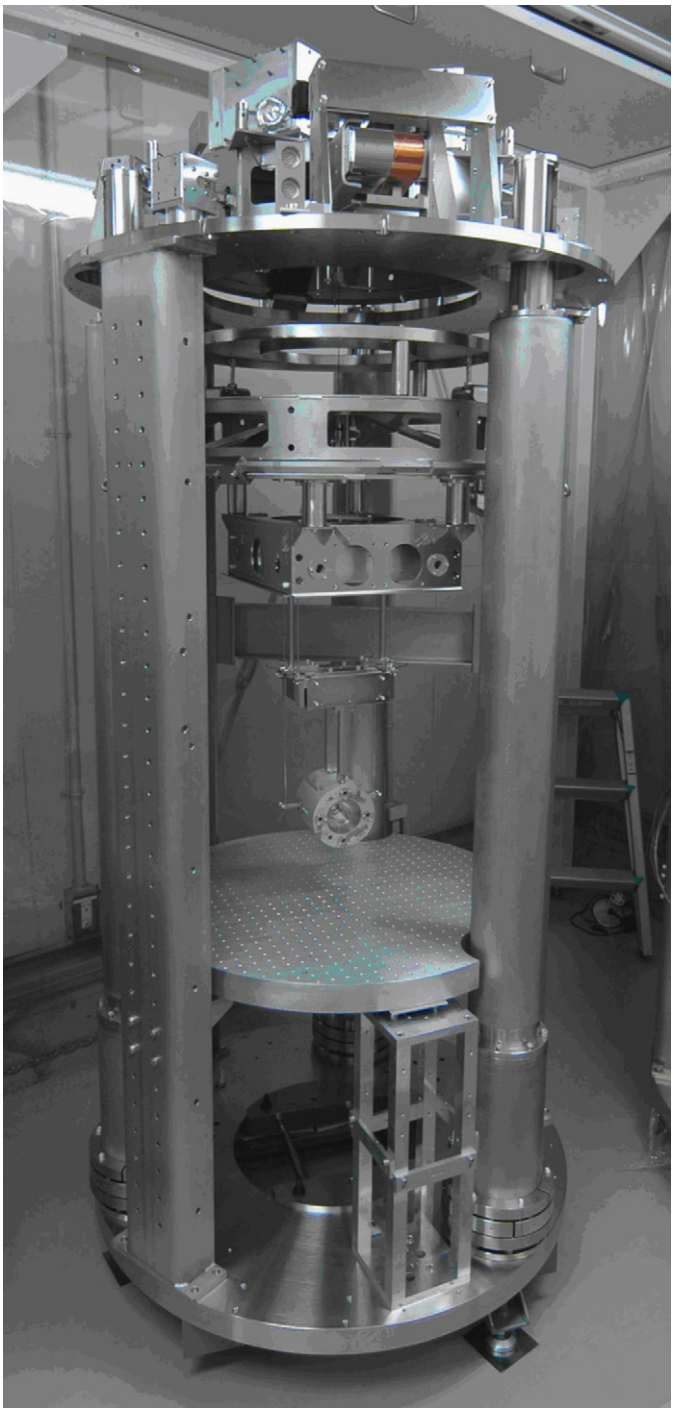

Fig. 10. IP TAMA-SAS as implemented.

Acknowledgments

We gratefully acknowledge the support of the United States National Science Foundation through Awards 0457528 and 0107417 and Columbia University in the City of New York. We thank the colleagues who have helped us along the way. Special thanks go to Gianni Gennaro of Promec for extremely effectively drafting all SAS design, and Carlo Galli of Galli&Morelli for the superb craftsmanship of our mechanical parts. We would like to thank Zsuzsa Márka, Benoit Mours, Giovanni Losurdo, Yoichi Aso and Gary Sanders for their insightful and useful reviews and comments.

This research was partially supported by the Japanese Ministry of Education, Science, Sports and Culture, Grant-in-Aid for Scientific Research on Priority Areas, 13048101, 2001-2005.

References

[1] A. Bertolini et al., New seismic attenuation system (SAS) for the LIGO advanced configurations (LIGO2), in: Proceedings of the1999 Amaldi Conference., Pasadena, CA, 1999.
[2] A. Takamori, et al., Class. Quantum Grav. 19 (2002) 1615.
[3] A. Takamori, G. Gennaro, T. Zelenova, R. DeSalvo, TAMA seismic attenuation system (SAS) mirror suspension system (SUS) mechanical drawings, LIGO-D-010250-00-R, 2001.
[4] M.V. PLissi, et al., Rev. Sci. Instrum. 6 (2000) 71.
[5] M. Barton, A. Bertolini, E. Black, G. Cella, E. Cowan, E. D'ambrosio, R. DeSalvo, K. Libbrecht, V. Sannibale, A. Takamori, N. Viboud, P. Willems, H. Yamamoto, Proposal of a Seismic Attenuation System (SAS) for the LIGO Advanced Configuration (LIGO-II), T990075-00, 1999, (LIGO Internal Note).
[6] A. Bertolini, G. Cella, W. Chenyang, R. DeSalvo, J. Kovalik, S. Márka, V. Sannibale, A. Takamori, H. Tariq, N. Viboud, Nucl.Instr.and Meth.A 461 (2001) 300.
[7] R. DeSalvo, et al., Nucl. Instr. and Meth. A 420 (1999) 316.
[8] G. Ballardin, et al., Rev. Sci. Instrum. 72 (9) (2001) 3643.
[9] G. Losurdo, et al., Rev. Sci. Instrum. 70 (1999) 2507.
[10] G. Losurdo, Ultra-low frequency inverted pendulum for the VIRGO test mass suspension, Ph.D.Thesis, Scuola Normale Superiore, Pisa, 1998. 〈http://www.virgo.infn.it/thesis/DottLosurdo.ps〉.

[11] J. Winterflood, D.G. Blair, Phys. Lett. A 243 (1998) 1.
[12] J. Winterflood, Z.B. Zhou, D.G. Blair, Ultra-low residual motion suspension system, in: Proc.Second TAMA Int. workshop on Gravitational Wave Detection (National Olympics Memorial Youth Center Tokyo, Japan October 19–22, 1999, Tokyo Universal Academy), 2001, pp. 301–310.
[13] J. Winterflood, D.G. Blair, B. Slagmolen, Phys. Lett. A 300 (2002) 122.
[14] G. Saul, et al., Source Book on Maraging Steels, American Society for Metals, Cleveland, 1979.
[15] V. Sannibale, Classical Mechanics Measurements: The Inverted Pendulum, Freshman Physics Laboratory (PH003), California Institute of Technology, California, 2001.
[16] A.L. Fetter, J.D. Waleczka, Theoretical Mechanics of Particles and Continua (Paperback), Dover Publications, New York, 2003 ISBM: 10:0486432610.
[17] A. Bertolini, High sensitivity accelerometers for gravity experiments, Ph.D.Thesis, Universita' di Pisa (2001), accelerometer details are available at LIGO-D-010240-00-R.
[18] C. Wang, H. Tariq, R. DeSalvo, Y. Iida, S. Márka, Y. Nishi, V. Sannibale, A. Takamori, Nucl. Instr. Meth. Res. A 489 (2002) 563.
[19] G. Losurdo, Inertial control of the Virgo superattenuators, in: Proceedings of the 1999 Amaldi Conference., Pasadena, CA, 1999.
[20] G. Losurdo, G. Calamai, E. Cuoco, L. Fabbroni, G. Guidi, M. Mazzoni, R. Stanga, F. Vetrano, Rev. Sci. Instrum. 72 (2001) 3653.
[21] H. Tariq, A. Takamori, Chenyang Wang, R. DeSalvo, A. Gennai, L. Holloway, G. Losurdo, S. Márka, F. Paoletti, D. Passuello, V. Sannibale, R. Stanga, Nucl. Instr. Meth. Res. A 489 (2002) 570.
[22] A. Takamori, Low frequency seismic isolation for gravitational wave detectors, Ph.D Thesis, LIGO-P-030049-00-R available at 〈http://admdbsrv.ligo.caltech.edu/dcc/〉.
[23] G. Cagnoli, et al., Phys. Lett. A 237 (1998) 21.
[24] M. Beccaria, et al., Nucl. Instr. Meth. A 404 (1998) 455.
[25] K. Arai, A. Takamori, Y. Naito, K. Kawabe, K. Tsubono, A. Araya, in: Proceedings of the TAMA International Workshop on Gravitational Waves Detection, Saitama, Japan, 1996.
[26] K. Tsubono, A. Araya, K. Kawabe, S. Moriwaki, N. Mio, Rev. Sci. Instrum. 8 (1993) 64.
[27] A. Takamori, A. Bertolini, G. Cella, E. D'ambrosio, R. DeSalvo, V. Sannibale, N. Viboud, in Proceedings of the Second TAMA InternationalWorkshop on Gravitational Wave Detection Tokyo, Japan, 1999.
[28] K. Kuroda, Astron.Herald 94/10 (2001) 472–478.
[29] D. Tatsumi, et al., Current status of Japanese detectors, in: Proceedings of the 11th Annual Gravitational Wave Data Analysis Workshop (GWDAW-11), Potsdam, Germany, 18–21 December 2006, to appear, e-Print: arXiv:0704.2881.